INTERNATIONAL JOURNAL OF SATELLITE COMMUNICATIONS
Int. J. Satell. Commun. **17**, 17–36 (1999)

Assessment of model-based scintillation variance prediction on long-term basis using Italsat satellite measurements

Frank S. Marzano[1]*, Carlo Riva[2], Alessio Banich[2] and Fabio Clivio[2]

[1]*Dipartimento di Ingegneria Elettrica, Università dell'Aquila, Monteluco di Roio, 67040 L'Aquila, Italy*
[2]*Dipartimento di Elettronica e Informazione, Politecnico di Milano, Piazza Leonardo da Vinci, 32 - 20133 Milano, Italy*

SUMMARY

The objective of this paper is to assess the accuracy of model-based statistical methods for predicting clear-air scintillation amplitude variance from ground-based meteorological measurements on long term basis. Six model-based estimation methods are considered and discussed, two of them including also the use of vertically integrated water vapour content as a predictor. They are derived from synthetic data, obtained by applying an electromagnetic model to a large historical radiosounding dataset in order to simulate the received scintillation power at microwave and millimeter-wave. The empirical methods of ITU-R, Karasawa, and Ortgies are also considered for comparison. The long-term predictions derived from each method are compared with measurements from the Italsat satellite beacons at 18·7, 39·6, and 49·5 GHz, acquired during 1995 at Spino d'Adda (Milan, Italy) site. The method intercomparison is carried out by checking the assumed best-fitting probability density function for the log-amplitude fluctuation variance and by applying the considered methods to the available ground-based meteorological measurements. Statistical results in terms of bias, root mean square value and skewness of the percentage error are discussed in order to understand the potential and the limits of each model-based prediction method within this case study.

KEY WORDS: scintillation; earth–satellite links; prediction methods; electromagnetic models

1. Introduction

In the last few years the rapid growth of fixed and mobile telecommunication services has put in evidence the increasing request of larger channel capacity.[1] These aspects have oriented the radiopropagation research to the exploitation of frequencies at Ka band and above.[2] At frequencies higher than 15 GHz, a microwave link crossing the atmosphere can be strongly affected by fading due to a combination of gas absorption and hydrometeor extinction, by depolarization due to atmospheric anisotropies and by scintillation.[3,4]

* Correspondence to: F. S. Marzano, Dipartimento di Ingegneria Elettrica, Università dell'Aquila, Monteluco di Roio, 67040 L'Aquila, Italy. E-mail: marzano@ing.univaq.it

Contract/grant sponsor: Italian Ministry of University and Scientific and Technological Research (MURST); Contract/grant sponsor: Italian Space Agency (ASI)

CCC 0737–2884/99/010017–20$17.50

Received October 1998
Accepted February 1999

Scintillation phenomena are attributed to atmospheric turbulence which induces refractive index inhomogeneities, thus causing time and space random variations of the amplitude, phase and angle of arrival of the transmitted signal.[5] Satellite–earth links are mainly affected by free-atmosphere and cloud-induced turbulence, while terrestrial links are predominantly caused by turbulence in the atmospheric boundary layer.[6] The scintillation intensity is proved to increase at higher frequencies, at lower elevation angles and with smaller receiving antennas. The renewed interest in scintillation studies is mainly due to their relevant impact on the performances of digital telecommunications with low margins for high availability. In future very-small aperture terminal (VSAT) communications systems at millimeter-waves, e.g. turbulence-induced scintillation cannot be neglected, especially at low elevation angles where long-term availability and performances are found to be influenced not only by rain effects, but also by scintillation.[7]

In the last decade some microwave propagation experiments, such as Olympus and Italsat, have been carried out to evaluate the impact of tropospheric scintillation and, in general, of atmospheric phenomena, on the budget design of earth–satellite links.[8] These experiments represent a unique opportunity to test statistical methods for predicting tropospheric scintillation directly from meteorological data at millimeter-wave.

In particular, many efforts have been recently devoted to the application of electromagnetic models, describing the interaction between microwave radiation and turbulent atmosphere, as a source for developing scintillation prediction methods.[9–12] The reason of this interest is due to the fact that they can provide a valuable tool to determine the received scintillation power and its spectrum in a given frequency band and for a given elevation angle. The prediction methods based on this modelling approach have, on one hand, the advantage to derive the scintillation statistics without needing satellite measurements for the considered site, but, on the other hand, strongly rely on the goodness of the interaction model used.[12]

The model-based prediction methods are generally trained by a large set of numerical outputs simulating the received scintillation power along a slant path through an intermittent turbulent stratified atmosphere described by a large vertical profiles of atmospheric variables, obtained by radiosonde balloons.[10,12] Actually, another valuable source of meteorological vertical profiles is represented by gridded data of numerical weather forecast services both at a macroscale (hundreds of km) and at a mesoscale (tens of km) spatial resolution. By means of polynomial regression techniques, the prediction methods statistically relate the simulated scintillation intensity to ground meteorological data, which are generally much more achievable than radiosonde data.[11] Recent investigations have also introduced the vertically integrated water vapour content, derivable from ground-based microwave radiometers or from Global Positioning Systems (GPS), as a further predictor.[12] Even though some of these model-based methods have been successfully compared with Olympus measurements,[11] there is a need to validate their potential by using satellite measurements in the 20–50 GHz band also with respect to more consolidated and popular empirical methods, such as ITU-R.[13]

In this paper, the objective is to assess the accuracy of six model-based statistical methods for predicting clear-air scintillation amplitude variance from ground-based meteorological measurements on long-term basis. These model-based methods and most commonly used empirical prediction methods are briefly reviewed in Section 2. The data processing of Italsat measurements at 18·6, 39·6, and 49·5 GHz and corresponding ground meteorological data, acquired during 1995 in Spino d'Adda (Milano, Italy), are described in Section 3. Finally, in Section 4 we test all the prediction methods by using the Italsat measurements on a monthly basis both at midday and

midnight, discussing the statistical results in terms of bias, root mean square value and skewness of the percentage error.

2. Model-based and empirical prediction methods

Throughout the text we have tried to use the word 'model' to mean atmospheric propagation models and the word 'method' to refer to the statistical prediction techniques. In the following subsections we will distinguish between the 'model-based' and the 'empirical' prediction methods. Both the approaches use the regression analysis to build a scintillation predictor. However, the distinction is due to the fact that, on the one hand, the model-based approaches use experimental meteorological variables derived from radiosounding observations (RAOBs), but scintillation variances derived from a propagation model. On the other hand, the empirical techniques use experimental meteorological data and experimental scintillation intensities. Thus, the main feature of the model-based approaches is to introduce an atmospheric propagation model to derive the regression coefficients of a scintillation prediction method.

Most statistical prediction methods usually relate the standard deviation, σ_χ or the variance, σ_χ^2 of the amplitude fluctuation, χ (dB) to surface meteorological measurements.[11–16] It can be convenient to define normalized quantities in order to unify the description of the prediction methods included in this work and to highlight their differences. This task is also facilitated by noticing that almost all the considered methods share a similar formulation, as it will be apparent later on.

Since the scintillation standard deviation or variance are usually normalized with respect to the antenna aperture averaging factor G, the frequency f(GHz), and the elevation angle θ, we can introduce a normalized scintillation variance $\sigma_{\chi\mathrm{n}}^2$ as follows:

$$\sigma_{\chi\mathrm{n}}^2 = \sigma_\chi^2 G^{-2} f^{-\alpha} (\sin\theta)^\beta \tag{1}$$

where α and β are the frequency scaling exponent and the elevation scaling exponent, respectively, and σ_χ^2 is conventionally expressed in dB^2. The antenna-aperture averaging factor G is generally a function of the antenna diameter and the effective path length in turbulence.[13,14] From (1) it is straightforward to deduce the relationship for the normalized scintillation standard deviation $\sigma_{\chi\mathrm{n}}$.

Referring to the log-normal probability density function (pdf) of the scintillation variance, the definition given in (1) implies that the normalized log-variance $\ln(\sigma_{\chi\mathrm{n}}^2)$ is expressed by

$$\ln(\sigma_{\chi\mathrm{n}}^2) = \ln(\sigma_\chi^2) + \ln[G^{-2} f^{-\alpha} (\sin\theta)^\beta] \tag{2}$$

where the log-variance $\ln(\sigma_\chi^2)$ is conventionally expressed in Nepers (Np).[12]

Notice that in the following text we will indicate the temporal averaging on long term basis by means of angle brackets, so that $\langle \sigma_{\chi\mathrm{n}} \rangle$ and $\langle \ln(\sigma_{\chi\mathrm{n}}^2) \rangle$ will stand for monthly-averaged normalized scintillation standard deviation and log-variance, respectively.

2.1. Model-based methods on long-term basis

Six statistical methods for the prediction of the monthly-averaged scintillation variance from ground measurements are briefly resumed here. They are based on numerical simulations of scintillation power as received by a beacon station where a large radiosounding data base is available. The physical model behind these simulations is the one developed by Tatarskii,[17]

refined for the intermittent turbulence hypothesis in References 9 and 10. Note that the local intermittence of the atmospheric turbulence is also taken into account in a statistical way by introducing the so-called intermittence factor (giving an index of the local atmospheric instability related to the wind velocity gradient and to the Richardson critical number) and estimating the local ensemble average of the scintillation variance. In practical applications, the local ensemble average is evaluated through a spatial average within a layer determined by the vertical resolution of the available radiosounding. Moreover, the radiosonde vertical sampling imposes also to discretize the integral expressions so that a layered atmosphere is considered.

For the numerical simulations in this work, a large database of radiosounding observations (RAOBs) with a vertical spatial resolution of about 150 m or smaller, performed in Milan over almost 10 years (twice a day around midday and midnight), has been examined.[11,12] An accurate selection of the clear-sky RAOBs has been carried out in order to exclude rainy conditions. For each meteorological profile set (i.e. temperature, pressure, relative humidity and wind vector), the refractive-index structure constant C_n^2 at each layer has been evaluated and the total received scintillation variance (power) σ_χ^2 has been calculated through the weak-fluctuation model for a given frequency, angle and antenna diameter.

The outputs of the above simulation consisted of 3655 received scintillation powers associated to the ground meteorological variables, to the vertically averaged structure constant C_n^2, and to the vertically integrated water vapour content. By applying the statistical regression analysis to the simulated data base, prediction formulas on an hourly basis and a monthly basis have been found depending on the regression model function used to relate the input surface variables to the predicted scintillation log-variance.

2.1.1. DPSP and MPSP methods. The Direct Physical-Statistical Prediction (DPSP) method is widely illustrated in Reference 11. It is based on the direct correlation between the monthly-average of the log-variance $\langle \ln(\sigma_{\chi n}^2) \rangle$ and the surface temperature $\langle T_s \rangle$ (°C). In order to match the definition given in (2), DPSP can be rewritten as

$$\langle \ln(\sigma_{\chi n}^2) \rangle = a_{01} + a_{11} \langle T_s \rangle \tag{3}$$

Referring to Eq. (1), it has been assumed $\alpha = 7/6 = 1{\cdot}166$ from the Tatarskii theory, while $\beta = 2{\cdot}40$ and the antenna aperture averaging factor G are given by ITU-R.[13] The coefficients of (3) are given in Table I.

The Modelled Physical-Statistical Prediction (MPSP) method differs from DPSP for the fact that a physical model to define the regression form is employed.[11] That is, if a thin-layer of homogeneous turbulent atmosphere is assumed, the problem can be analytically solved and expressed by a simple formula relating the scintillation variance to the layer parameters.[12,17] In order to match the definition given in (2), MPSP can be stated as

$$\langle \ln(\sigma_{\chi n}^2) \rangle = a_{02} + a_{12} \langle T_s \rangle + a_{22} \ln(a_{32} + a_{42} \langle T_s \rangle) \tag{4}$$

where the expression inside the parenthesis represents an estimate of the turbulent layer height. Referring to (2), it also gives $\alpha = 7/6 = 1{\cdot}166$ and $\beta = 11/6 = 1{\cdot}833$ consistently with the Tatarskii theory, while the factor G is the one given by ITU-R. The coefficients of (4) are given in Table I.

2.1.2. STH2 and STN2 methods. From the same synthetic data set used for DPSP and MPSP, non-linear prediction methods have been also derived. The analysis of statistical simulated tests shows that the best regressive estimators on long-term basis have a quadratic form and are based

Table I. Regression coefficients of each of the considered prediction methods, named in the first column and expressed by the equation listed in the second column. The term 'coef_i' refers to the coefficients '$a_{i1}, a_{i2}, \ldots, e_{i1}, e_{i2}$' of each equation, while the symbol '×' indicates the absence of the corresponding variable

Method	Eq.	coef_0	coef_1	coef_2	coef_3	coef_4	coef_5	coef_6
DPSP	(3)	−11·0095	0·1235	×	×	×	×	×
MPSP	(4)	−24·9053	0·0684	1·8333	2058	94·5	×	×
STH2	(5)	−14·9504	0·1546	0·0747	−0·0011	−0·0005	×	×
STN2	(6)	−12·3889	0·1300	0·0151	−0·0016	0·0000	×	×
STHV2	(7)	−15·0762	0·1473	0·0772	0·0133	−0·0006	−0·0005	−0·0007
STNV2	(8)	−12·4255	0·1226	0·0076	0·0427	−0·0013	0·0001	−0·0014
Karasawa	(9)	0·00342	0·0001186	×	×	×	×	×
ITU-R	(10)	0·00360	0·0001030	×	×	×	×	×
Ortgies-T	(11)	−12·50	0·0865	×	×	×	×	×
Ortgies-N	(12)	−13·45	0·0462	×	×	×	×	×

either on surface temperature $\langle T_s \rangle$ (°C) and relative humidity $\langle \mathrm{RH_s} \rangle$ (expressed conventionally in per cent) for the STH2 method or on surface temperature and wet-refractivity $\langle N_{ws} \rangle$ (expressed conventionally in per cent) for the STN2 method.[12] The formula to compute $\langle N_{ws} \rangle$ used here is the one given in Reference 14, i.e.: $\langle N_{ws} \rangle = 3730 \langle \mathrm{RH_s} \rangle \langle e_s \rangle / (\langle T_s \rangle + 273)^2$ with $\langle e_s \rangle$ the surface saturated-vapour pressure (mb). It is worth mentioning that most of the prediction algorithms proposed in literature give formulas based on either temperature or wet-refractivity in linear form. Moreover, the prediction methods have been derived not only for the monthly-averaged quantities, but also for the hourly averaged quantities.

Referring to (2), the STH2 method has the following expression on a monthly basis:[12]

$$\langle \ln(\sigma^2_{\chi n}) \rangle = b_{01} + b_{11} \langle T_s \rangle + b_{21} \langle \mathrm{RH_s} \rangle + b_{31} \langle T_s \rangle^2 + b_{41} \langle \mathrm{RH_s} \rangle^2 \tag{5}$$

Correspondingly, the STN2 method is given by on a monthly basis:[12]

$$\langle \ln(\sigma^2_{\chi n}) \rangle = b_{02} + b_{12} \langle T_s \rangle + b_{22} \langle N_{ws} \rangle + \mathrm{b}_{32} \langle T_s \rangle^2 + b_{42} \langle N_{ws} \rangle^2 \tag{6}$$

For both STH2 and STN2 it is assumed $\alpha = 7/6 = 1{\cdot}166$ and $\beta = 11/6 = 1{\cdot}833$ consistently with the Tatarskii theory, while the factor G is the one given by ITU-R. The coefficients of (5) and (6) are given in Table I.

2.1.3. STHV2 and STNV2 methods. A further extension of the STH2 and STN2 methods has been also investigated in Reference 12. The rationale is related to the fairly good correlation between the normalized scintillation log-variance and the vertically integrated water vapour $\langle V_c \rangle$ (kg m^{-2} or mm), shown by simulated and experimental tests. This gives the possibility to estimate σ^2_χ from a combination of surface temperature $\langle T_s \rangle$, relative humidity $\langle \mathrm{RH_s} \rangle$ (or wet refractivity $\langle N_{ws} \rangle$) and integrated water vapour $\langle V_c \rangle$. Thus, by applying the multivariate statistical regression method, the following relationship has been derived on a monthly basis for the STHV2 method[12]

$$\langle \ln(\sigma^2_{\chi n}) \rangle = c_{01} + c_{11} \langle T_s \rangle + c_{21} \langle \mathrm{RH_s} \rangle + c_{31} \langle V_c \rangle + c_{41} \langle T_s \rangle^2 + c_{51} \langle \mathrm{RH_s} \rangle^2 + c_{61} \langle V_c \rangle^2 \tag{7}$$

and correspondingly, for the STNV2 method (not explicitly given in Reference 12):

$$\langle \ln(\sigma_{\chi n}^2) \rangle = c_{02} + c_{12}\langle T_s \rangle + c_{22}\langle N_{ws} \rangle + c_{32}\langle V_c \rangle + c_{42}\langle T_s \rangle^2 + c_{52}\langle N_{ws} \rangle^2 + c_{62}\langle V_c \rangle^2 \tag{8}$$

For both STHV2 and STNV2 it is assumed $\alpha = 7/6 = 1{\cdot}166$ and $\beta = 11/6 = 1{\cdot}833$ consistently with the Tatarskii theory, while the factor G is the one given by ITU-R. The coefficients of (7) and (8) are given in Table I.

2.2. Empirical methods on long-term basis

The following prediction methods are based on experimental measurements recorded at ground-stations along satellite microwave links. They are briefly recalled both for completeness and to show the similarities and the differences with respect to the model-based methods, described above. Moreover, they will give a valuable term of comparison when testing the prediction methods by using the Italsat measurements.

2.2.1. Karasawa and ITU-R methods. The method proposed in Reference 14, hereinafter for simplicity called 'Karasawa method', is assumed to be valid for frequencies ranging from 7 to 14 GHz and elevation angles ranging from 4° to 30°. The regression between the monthly-averaged normalized value $\langle \sigma_{\chi n} \rangle$ (dB) and the surface wet-term refractive index $\langle N_{ws} \rangle$ (expressed conventionally in per cent) is given by[14]

$$\langle \sigma_{\chi n} \rangle = d_{01} + d_{11}\langle N_{ws} \rangle \tag{9}$$

Referring to the definition given in (1), it holds $\alpha = 0{\cdot}90$ (i.e. 0·45 for $\langle \sigma_{\chi n} \rangle$) and $\beta = 2{\cdot}60$ (i.e. 1·30 for $\langle \sigma_{\chi n} \rangle$) with the factor G reported in Reference 14. The coefficients of (9) are given in Table I.

The International Telecommunication Union method, described in Reference 13 and hereinafter for brevity cited as 'ITU-R method', is mostly derived from the previous Karasawa method, but applicable to frequencies ranging also from 7 to 14 GHz and characterized by the following expression[13]

$$\langle \sigma_{\chi n} \rangle = d_{02} + d_{12}\langle N_{ws} \rangle \tag{10}$$

Referring to (1), it is assumed that $\alpha = 1{\cdot}16$ (i.e. 0·58 for $\langle \sigma_{\chi n} \rangle$) and $\beta = 2{\cdot}40$ (i.e. 1.20 for $\langle \sigma_{\chi n} \rangle$), while the factor G is given in Reference 13. The coefficients of (10) are again given in Table I.

2.2.2. Ortgies-T and Ortgies-N methods. The methods proposed by Ortgies are derived from Olympus measurements in Darmstadt using the beacons at 12·5, 20 and 30 GHz and antennas with diameters of 0·6, 1·8 and 3·7 m, respectively.[15,16] They are applicable for elevation angles from 6·5° to 30° and two linear relations between monthly mean value of $\ln(\sigma_\chi^2)$ and surface meteorological variables are proposed.

The first method uses the monthly surface temperature $\langle T_s \rangle$ (°C) as a predictor and is given by (hereinafter, called 'Ortgies-T method')[15]

$$\langle \ln(\sigma_{\chi n}^2) \rangle = e_{01} + e_{11}\langle T_s \rangle \tag{11}$$

while the second one relates the monthly log-variance to the surface wet refractivity $\langle N_{ws} \rangle$ (expressed conventionally in per cent) as follows (hereinafter, called 'Ortgies-N method')[16]

$$\langle \ln(\sigma_{\chi n}^2) \rangle = e_{02} + e_{12}\langle N_{ws} \rangle \tag{12}$$

Referring to the definition given in (2), both for Ortgies-T and Ortgies-N methods, it is assumed $\alpha = 1{\cdot}21$ and $\beta = 2{\cdot}40$, while the factor G is the one given by ITU-R. The coefficients of (11) and (12) are given in Table I.

3. Italsat measurements and meteorological data

The experimental data used in this work have been taken at the ground-station of Spino d'Adda (Milan, Italy) along the down-link of Italsat-F1 satellite, launched in January 1991 on a geostationary orbit at longitude 13.2°E. The Italsat-F1 is still providing three beacons at 18·7 GHz with vertical polarization (hereinafter, also called 20 GHz channel), 39·6 GHz with circular polarization (hereinafter, also called 40 GHz channel), and 49·5 GHz with vertical and horizontal polarization (hereinafter, also called 50 GHz channel). The Spino d'Adda station is one of three main Italian ground-stations and operates at an elevation angle of 37·8° with antennas of 3·5 m.[8] The purposes of the Italsat experiment are basically oriented to radiopropagation studies: signal fading, depolarization, and scintillation; measurements of inter-band phase; amplitude and phase distortion at 40 GHz over a band of ± 505 MHz; and characterization of the 50 GHz channel. In July, 1997 the Italsat-F2 has been also successfully launched, even though carrying only the 20 GHz channel transponder.

3.1. Beacon and meteorological data processing

For this work 12 months of Italsat data have been available from 1 January 1995 to 31 December 1995 for the three beacons, acquired at a sampling rate of 1 Hz. A clear-sky threshold of $-1{\cdot}5$ dB has been applied to the log-amplitude time series of the 20-GHz copolar channel in order to select clear-air events. Thereafter, the Italsat signal has been filtered by applying an eight-order Butterworth high-pass filter with a cut-off frequency at -3 dB of 0·01 Hz. All the computed values of scintillation log-amplitude and variance have been then resampled every 1 min for recording.

In Spino d'Adda the meteorological data, consisting of surface temperature and relative humidity, were measured every 10 min. Only the meteorological measurements corresponding to the above-cited clear-sky periods have been retained. Three radiometric channels at 13·0, 23·8, and 31·6 GHz, and a raingage were also available at the same site. They were used to detect the presence of clouds and rain. Moreover, from 23·8 and 31·6 GHz channels the integrated water vapour $\langle V_c \rangle$ on a monthly basis was derived by using the estimation method proposed in Reference 12.

In order to make the beacon measurements consistent with the model-based predictors, derived from RAOB data set available twice a day, each available time series has been windowed around midday and midnight, choosing a period of about 45 min corresponding to the ascending time of a RAOB balloon. This reduction of the amount of available Italsat data has not significantly modified the statistical distribution of the log-amplitude scintillation variance. Monthly averages of these windowed measurements were performed, separately for midday and midnight data, thus providing 24 monthly mean values.[19]

Figure 1 shows the monthly-averaged Italsat log-variances (left panels) at 20, 40, and 50 GHz at midday and midnight, as a function of the month index. Analogously, the right panels of the same figure show the surface temperature, the surface wet refractivity, and the vertically integrated water vapour content against the month index. Figure 2 is the scatterplot between the

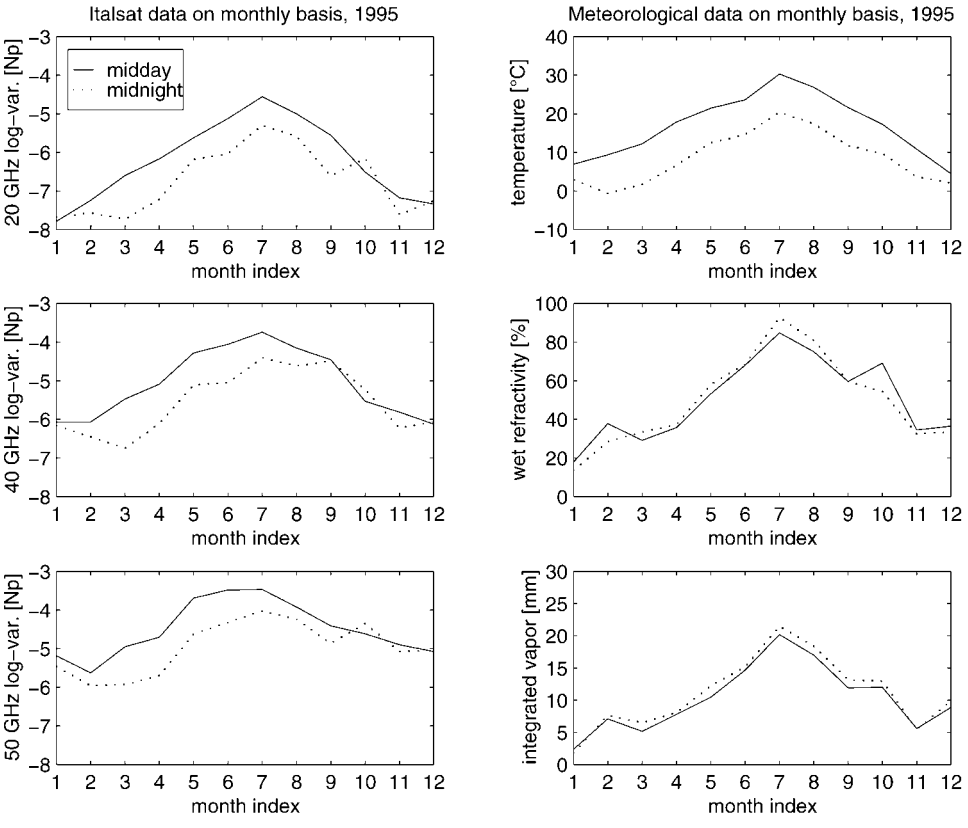

Figure 1. Monthly-averaged Italsat log-variance on left panels at 20 GHz (top panel), 40 GHz (middle panel), and 50 GHz (bottom panel) at midday and midnight, as a function of the month index (i.e. 1 is for January and 12 for December), measured at Spino d'Adda during 1995. Right panels show the corresponding surface temperature (top panel), surface wet refractivity (middle panel), and vertically integrated water vapour content (bottom panel) as a function of the month index. Midday and midnight data are indicated by solid and dashed lines, respectively

Italsat log-variances at 20, 40, and 50 GHz as a function of surface temperature (left panels), surface wet refractivity (middle panels), and vertically integrated water vapour content (right panels).

We have chosen to represent the scintillation log-variance, instead of its variance or standard deviation value, since all the model-based prediction methods use it as a diagnostic variable. Note that in order to get the variance value it is not correct to take simply the exponential of the log-variance value due to the presence of the monthly averaging, represented by the angle brackets in our notation (see (3), for example).

As expected, scintillation on long-term basis mostly follows the variation of surface temperature, being the intensity higher at midday than at midnight and lower in winter than in summer (up to one order of magnitude). The 'worst' case results to be the midday period during July; the results for the month of October are affected by a lack of Italsat data due to calibration failures in the receiving system. The fact that wet refractivity is inversely proportional to

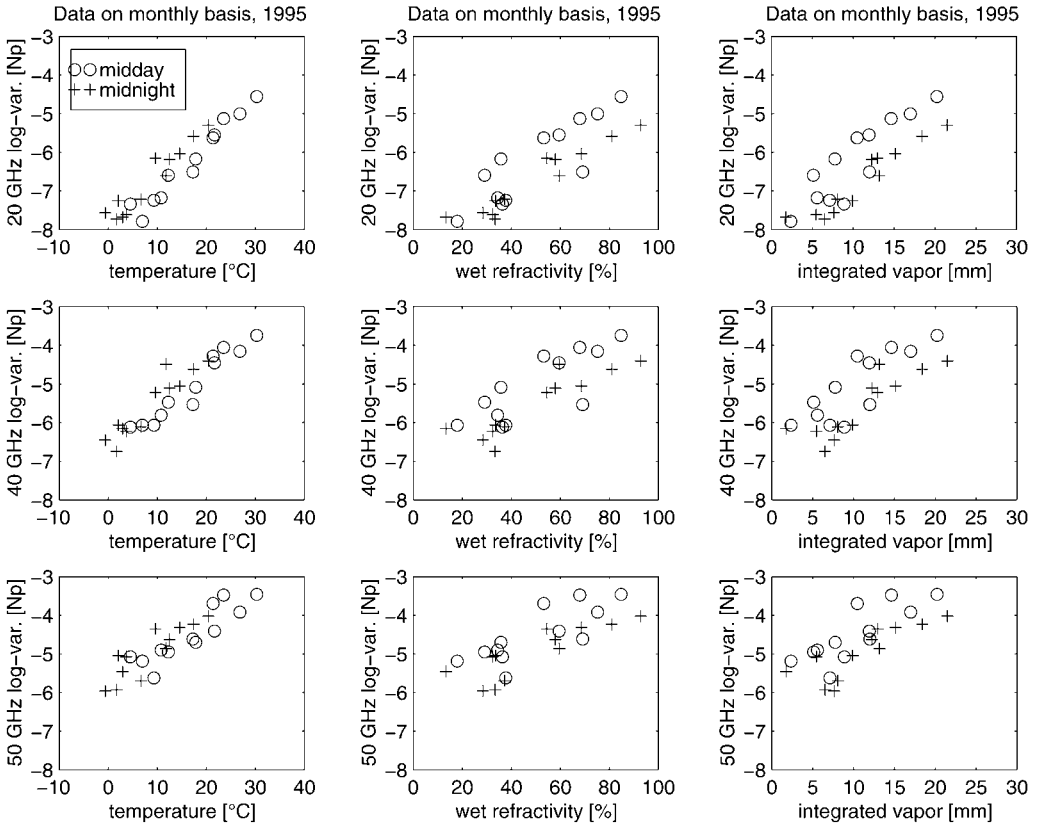

Figure 2. Monthly-averaged Italsat log-variance at 20 GHz (top panel), 40 GHz (middle panel), and 50 GHz (bottom panel) as a function of surface temperature (top panel), the surface wet refractivity (middle panel), and the vertically integrated water vapour content (bottom panel). Midday and midnight data are indicated by circle and cross symbols, respectively

temperature explains the slightly higher values of $\langle N_{ws} \rangle$ at midnight (when temperature is lower) with respect to those at midday (when temperature is higher). The behaviour of the integrated water vapour can be justified by considering the diurnal moisture flux from the heated soil.[18] It is worth mentioning about the high correlation between the measured log-variance and integrated water-vapour content: this is the main reason why its introduction into prediction models can give useful information.

4. Comparison of prediction methods with Italsat data

The considered prediction methods propose various formulas relating the scintillation parameters to ground-based meteorological measurements. Note that the model-based methods and the Ortgies methods provide estimates in terms of scintillation log-variance, while the Karasawa and ITU-R methods in terms of scintillation intensity.

4.1. Statistical distribution of scintillation variance

Before carrying out the prediction intercomparison, it is interesting to analyse which is the statistical distribution which better fits the sampled Italsat data.

A well established hypothesis is to assume that the log-amplitude fluctuation χ (dB) is stationary on a short term (order of a few minutes) and is described by a Gaussian probability density function. However, over a longer period of time the standard deviation or the variance σ_χ^2 of χ varies according to its own pdf. Based on theoretical and experimental works, the common assumption is to use a Gamma pdf for the scintillation intensity and a log-normal pdf for the scintillation variance.

Figure 3 shows the cumulative distribution function (cdf) of Italsat scintillation variance at 20, 40, and 50 GHz on a monthly basis around midday (left panels) and midnight (right panels) during summer. The log-normal distribution function, having the same mean and variance of the

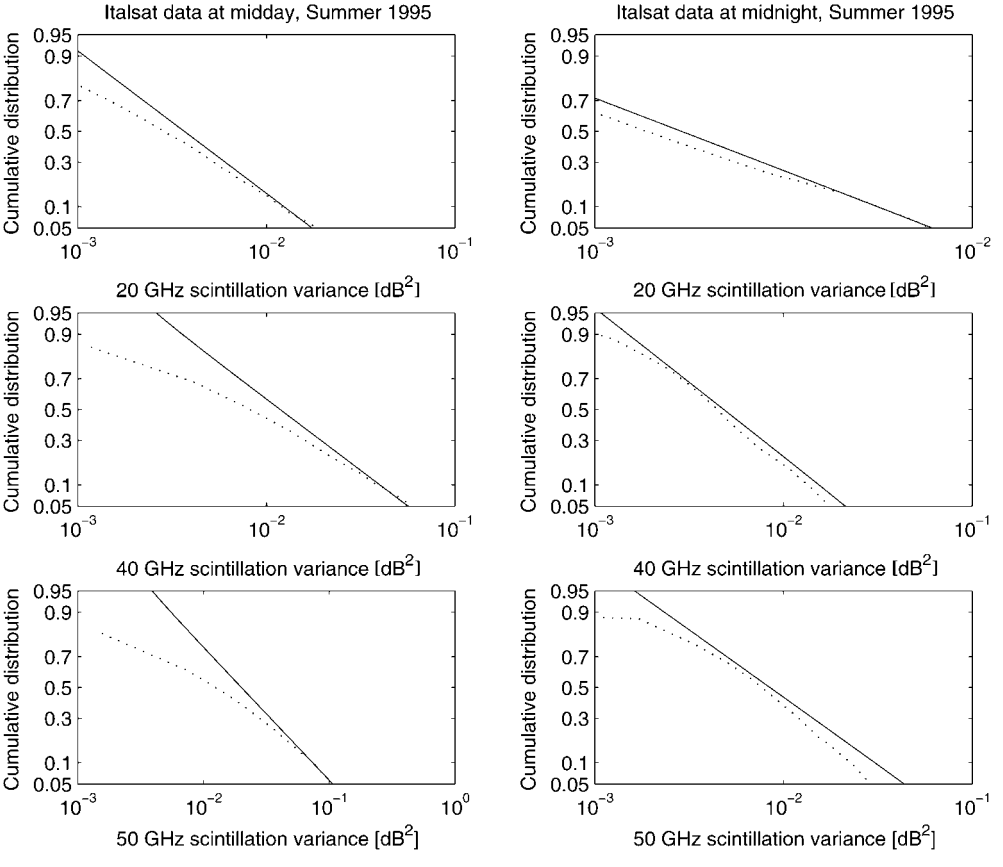

Figure 3. Cumulative distribution function of Italsat scintillation variance, plotted on a Gaussian scale and indicated by a solid line, at 20 GHz (top panel), 40 GHz (middle panel), and 50 GHz (bottom panel) on a monthly basis at midday (left panels) and midnight (right panels). The log-normal distribution function is also shown for comparison by a dashed line

measured data, is also shown for comparison. On the vertical axis a Gaussian scale has been used so that a log-normal cdf would result in a straight line.

According to our results, the log-normal distribution seems to fit the long term variations of σ_χ^2 during midnight at 20, 40, and 50 GHz and at 20 GHz during midday. Discrepancies are noted at 40 and 50 GHz for variance values less than 10^{-2} dB^2, probably caused by some effects of angle-of-arrival variations due to the large receiving antennas. These results are also consistent with the theoretical distribution derived in Reference 12 from synthetic data. Moreover, while Gamma pdf has proved to be suitable for low elevation angles and humid areas,[13] log-normal pdf is generally more adequate for high elevation angle and continental regions, like the Spino d'Adda site.[11]

It is also clear why the use of scintillation log-variance, instead of the variance or the standard deviation, is preferable in this context. Finally, the fact that we have found a very typical result for the scintillation variance cdf also suggests that our sampling of Italsat data around midnight and midday has not drastically changed the statistical characteristics of the considered data set.

4.2. Long-term prediction on a monthly basis

In order to perform the method intercomparison, we have defined a percentage fractional error ε_f as follows: $\varepsilon_f = 100(x_{meas} - x_{est})/x_{meas}$, where x_{meas} and x_{est} are the measured and the estimated variables under consideration, respectively. Besides the (linear) correlation coefficient between x_{meas} and x_{est}, we have characterized the fractional error ε_f in terms of its mean value (i.e. bias), its root mean square value (i.e. rms error) and its skewness factor.

The latter figure of merit measures the asymmetry of the error probability density function (pdf), being the difference between its mean and modal values, normalized to the standard deviation (e.g. the normal pdf has zero skewness). Positive values of skewness indicate that, for positive error values, the tail of the pdf is much longer at the right-hand side of the maximum (modal) value than at its left-hand side, and vice versa.

In this paragraph we will illustrate the results of the comparison between Italsat data and predicted values, discussing the statistical features of the percentage fractional error.

Figure 4 shows the monthly-averaged scintillation log-variance $\langle \ln(\sigma_\chi^2) \rangle$, estimated by means of DPSP (left panels) and MPSP (right panels) methods at 20, 40, and 50 GHz, as compared to the corresponding Italsat measurements. Figures 5 and 6 show the same as in Figure 4, but for the quadratic prediction methods grouped as STH2 and STN2, and as STHV2 and STNV2, respectively. Figure 7 shows the same as in Figure 4, but for Ortgies-T and Ortgies-N methods.

Figure 8 shows the comparison between monthly-averaged scintillation standard deviation (dB), estimated by means of Karasawa (left panels) and ITU-R (right panels) methods at 20, 40, and 50 GHz, and the corresponding Italsat measurements. Of course, in this case the temporal averaging has been applied to scintillation time series regenerated in terms of standard deviation values.

Tables II–IV show the bias, the rms value, and the skewness of the percentage fractional error plus the correlation coefficient between the estimated and measured scintillation on monthly basis for the ten prediction methods considered in this work at 20, 40, and 50 GHz, respectively. The results relative to bias, rms value, and skewness of the percentage fractional error, described in the tables, are visually summarized by the bar diagram shown in Figure 9, where they are grouped for each prediction method listed in the x-co-ordinate.

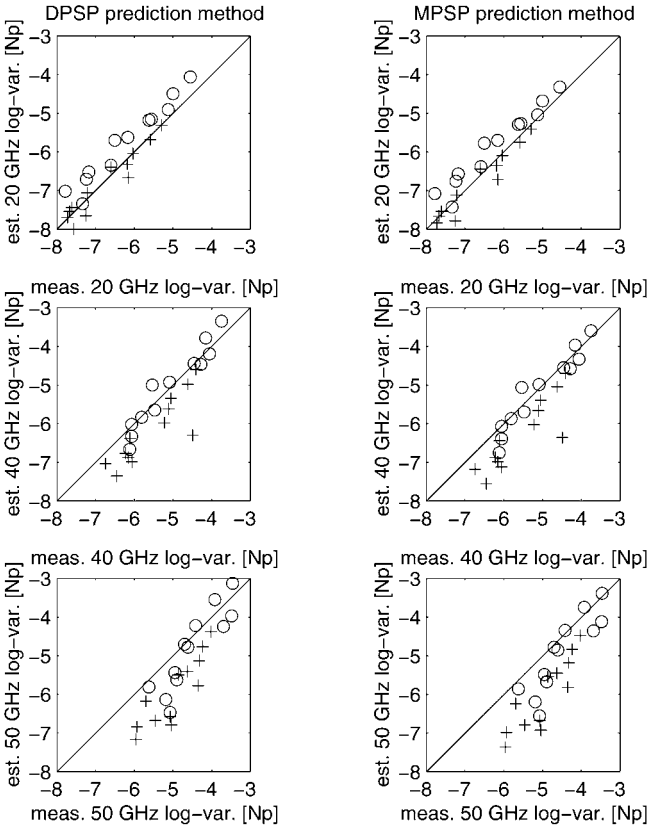

Figure 4. Monthly-averaged scintillation log-variance, estimated by means of the DPSP (left panels) and MPSP (right panels) methods at 20 GHz (top panel), 40 GHz (middle panel), and 50 GHz (bottom panel), as compared to the corresponding Italsat measurements. Midday and midnight data are indicated by circle and cross symbols, respectively

By analysing the results in terms of correlation coefficients, it emerges that the method with the highest values is the STNV2 one for all the Italsat channels, followed by the good score of the STN2 method. Among the empirical methods, the best one is the Ortgies-T method, while the others have correlation values less than 0·90, 0·75, 0·80 at 20, 40, and 50 GHz, respectively.

At 40 GHz the correlation values are less than both 20 and 50 GHz, a fact probably due to some problems in the channel calibration over the ± 505 MHz band and to an increase of noise in the channel chain. In general, we could say that for each prediction method the correlation values decrease with frequency, due to the appearance of strong non-linearities in the scintillation phenomena which are not easily accounted for in the estimation. In this respect, it is worth mentioning that the non-linear model-based methods seem to be able to better follow this feature typical of millimeter-wave propagation in turbulent atmosphere.

The analysis of the rms errors at 20 GHz shows a result which is different from that at 40 and 50 GHz. In fact, the STNV2 method shows a relatively high rms value (even though less than 10 per cent), while at 40 and 50 GHz it still performs better than the others. In terms of error

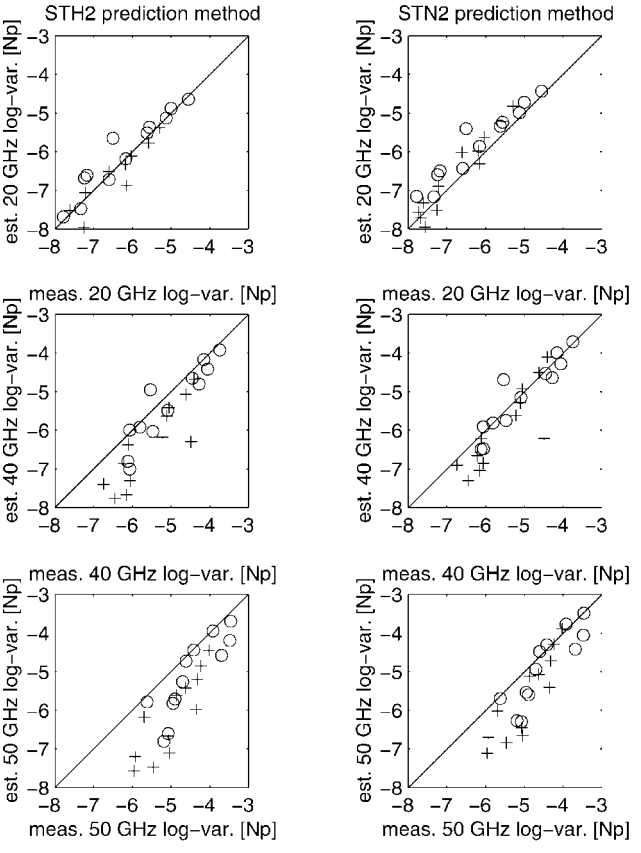

Figure 5. As in Figure 4, but for the STH2 and STN2 methods

standard deviation, that is if we centre the error with respect to its mean value, this anomaly is removed. In fact, by looking at the values of the error bias, we realize that STNV2 has one of the largest values at 20 GHz (about −6 per cent). The fact that at 40 and 50 GHz the biases of the model-based methods are still fairly low (less than 15–20 per cent) indicates that introducing non-linearity into statistical prediction not necessarily implies an increase of the error bias (as generally can happen).

The model-based prediction methods show an overall rms value less than 10, 30, and 20 per cent at 20, 40, and 50 GHz, much better than the empirical ones. Actually, the Ortgies methods performs quite well at 20 GHz, while at 40 and especially at 50 GHz denotes the limits of its assumptions. The ITU-R and the Karasawa methods surprisingly show better results at 50 GHz than at 20 GHz. This behaviour might be explained by the high value of the elevation angle exponent β (equal to 2·40, greater than the theoretical value 1·83) and by the fact that a logarithmic relation between variance and meteorological variables (as those used by Ortgies and model-based methods) is more suitable to estimate low scintillation intensities.

The error biases are predominantly negative at 20 GHz, while positive both at 40 and 50 GHz. This consideration can be usefully coupled with the analysis of the skewness values. First of all, we

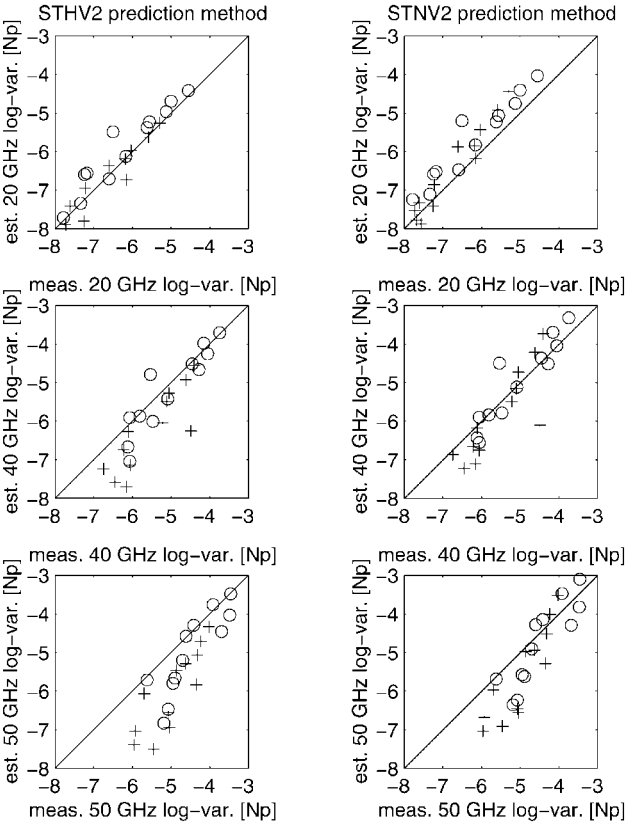

Figure 6. As in Figure 4, but for the STHV2 and STNV2 methods

notice that only in a few cases the skewness is zero or very small (less than 5 per cent). This implies that the error pdf cannot be considered Gaussian and statistical moments higher than the second one (variance) should be considered in order to completely characterize its behaviour.

The fact that the error pdf is not normal must not necessarily be viewed as a penalty. A positive skewness means that the maximum occurrence of errors is more concentrated towards zero, but having a relatively higher probability of large errors (corresponding to a longer pdf tail) and vice versa with a negative skewness. From an application point of view, the fact to disregard possible non-zero skewness values can have an impact on the budget design when considering the validity bounds of the link statistical models. For a given mean and standard deviation value of the error pdf, imposing a symmetric Gaussian error pdf in the presence of non-zero skewness can lead to overestimate the maximum error value and underestimate its occurrence in case of a positive skewness error (mean greater than mode value), while the opposite happens in case of negative skewness errors (mean smaller than mode).

Except for the ITU-R and Karasawa methods, the skewness values at 20 and 50 GHz are generally less than 20 and 40 per cent, respectively. Values larger than 200 per cent at 40 GHz are probably affected by the above mentioned calibration problems and the overall results at 40 GHz

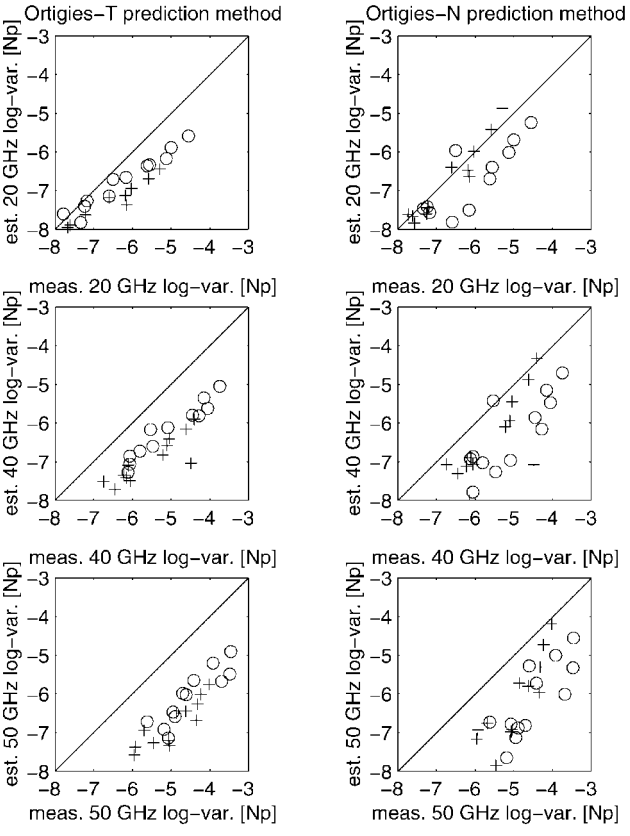

Figure 7. As in Figure 4, but for the Ortgies-T and Ortgies-N methods

are compensated by the small values of bias. Note that all the prediction methods, with the exception of Ortgies-N, show a positive skewness, while at 20 GHz the behaviour is highly variable.

We can conclude that the model-based prediction methods show performances generally better than the empirical techniques such as Ortgies, Karasawa, and ITU-R, which indeed have not been tuned to millimeter-wave and high-elevation angle applications. The performances at higher frequencies are generally worse than at 20 GHz, even though still less than 25 per cent in terms of percentage error. It is worth mentioning that the impact of adding the integrated water vapour as a predictor in the model-based methods, further improves the final accuracy especially at 40 and 50 GHz.

A final note regards the frequency scaling exponent in equations (1) and (2), which has been also experimentally derived from Italsat measurements. On a monthly basis it has been found that for the Spino d'Adda site the average values of α are about 1·93, 2·28, and 2·94 for 20/40, 20/50, and 40/50 channel ratios during the day and 1·97, 2·23, and 3·12 for 20/40, 20/50, and 40/50 channel ratios during the night. Considering that the common values of α go from 0·90 to 1·21, it is clear that these experimental values (with an average of 2·1) are almost double. The promising good

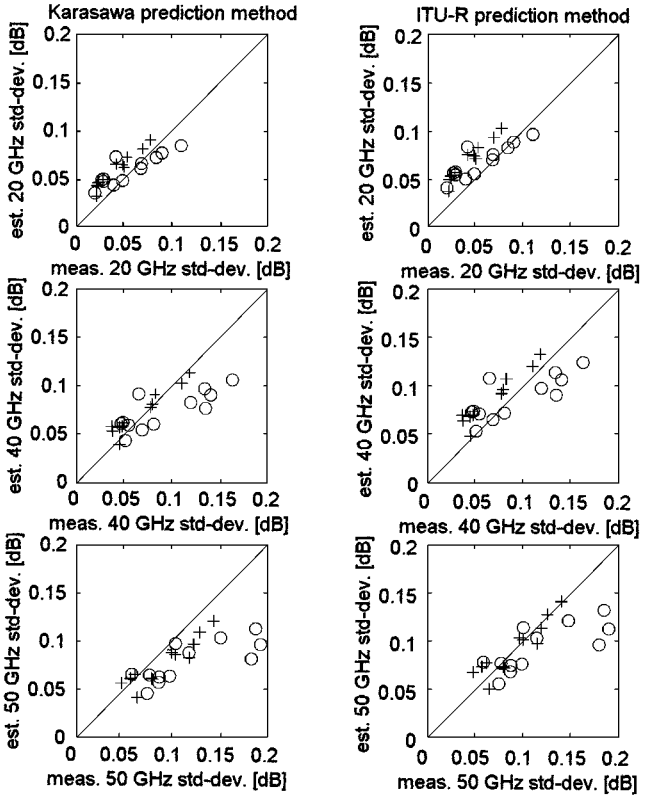

Figure 8. Monthly-averaged scintillation standard deviation, estimated by means of the Karasawa (left panels) and ITU-R (right panels) methods at 20 GHz (top panel), 40 GHz (middle panel), and 50 GHz (bottom panel), as compared to the corresponding Italsat measurements. Midday and midnight data are indicated by circle and cross symbols, respectively

Table II. Bias, rms value, and skewness of the percentage fractional error together with the correlation coefficient between estimated and measured scintillation intensity at 20 GHz on a monthly basis for the ten prediction methods, considered in this work

Method	Bias	rms value	Skewness	Correlation
DPSP	− 3·24	6·58	21·87	0·942
MPSP	− 1·64	5·78	20·30	0·938
STH2	0·72	5·92	2·87	0·932
STN2	− 4·53	6·64	− 19·23	0·952
STHV2	− 1·22	6·07	3·57	0·937
STNV2	− 6·66	8·91	− 14·76	0·959
Karasawa	35·32	50·58	93·92	0·851
ITU-R	63·98	79·14	76·42	0·851
Ortgies-T	10·48	10·66	− 20·56	0·943
Ortgies-N	6·16	12·94	11·07	0·871

Table III. Same as in Table II, but at 40 GHz

Method	Bias	rms value	Skewness	Correlation
DPSP	8·82	26·44	233·44	0·783
MPSP	10·80	27·01	233·22	0·786
STH2	13·78	28·60	181·34	0·777
STN2	7·01	23·23	208·25	0·808
STHV2	11·30	27·02	170·35	0·779
STNV2	4·30	22·62	154·19	0·809
Karasawa	− 5·83	30·23	339·55	0·491
ITU-R	16·59	40·90	344·31	0·491
Ortgies-T	29·32	41·25	308·82	0·782
Ortgies-N	23·57	34·76	80·08	0·732

Table IV. Same as in Table II, but at 50 GHz

Method	Bias	rms value	Skewness	Correlation
DPSP	13·18	18·02	− 0·08	0·887
MPSP	15·35	19·40	17·59	0·886
STH2	18·63	22·49	31·05	0·870
STN2	11·42	15·98	29·91	0·890
STHV2	15·97	20·59	30·95	0·871
STNV2	8·56	15·76	12·80	0·890
Karasawa	−23·23	29·23	125·20	0·759
ITU-R	−4·84	21·85	125·17	0·759
Ortgies-T	36·65	38·78	12·81	0·887
Ortgies-N	30·88	34·70	− 3·77	0·782

agreement between predicted and measured scintillation intensities found in this case study, even using frequency scaling exponents quite different from the empirical ones, should indicate that the model-based prediction methods (but also the Ortgies techniques) are fairly robust with respect to uncertainties about the α parameter. However, a deeper insight into this topic must be gained in the future.

5. Conclusions

The potential of model-based prediction methods is due to their flexibility in tuning the estimation relationships to a given site where a meteorological-profile archive is available without needing experimental beacon measurements.

The model-based approaches have some appealing advantages with respect to the empirical ones: (i) radiosounding data are more frequent in time and space and achievable than earth–satellite link data; (ii) even though radiosoundings are not available in a given site, it is possible to use gridded meteorological profiles derived from numerical weather forecasts; (iii) diverse frequency bands and elevation angles can be easily simulated; (iv) a thorough analysis of the radiation–turbulence interaction can be carried out. Moreover, model-based regressive

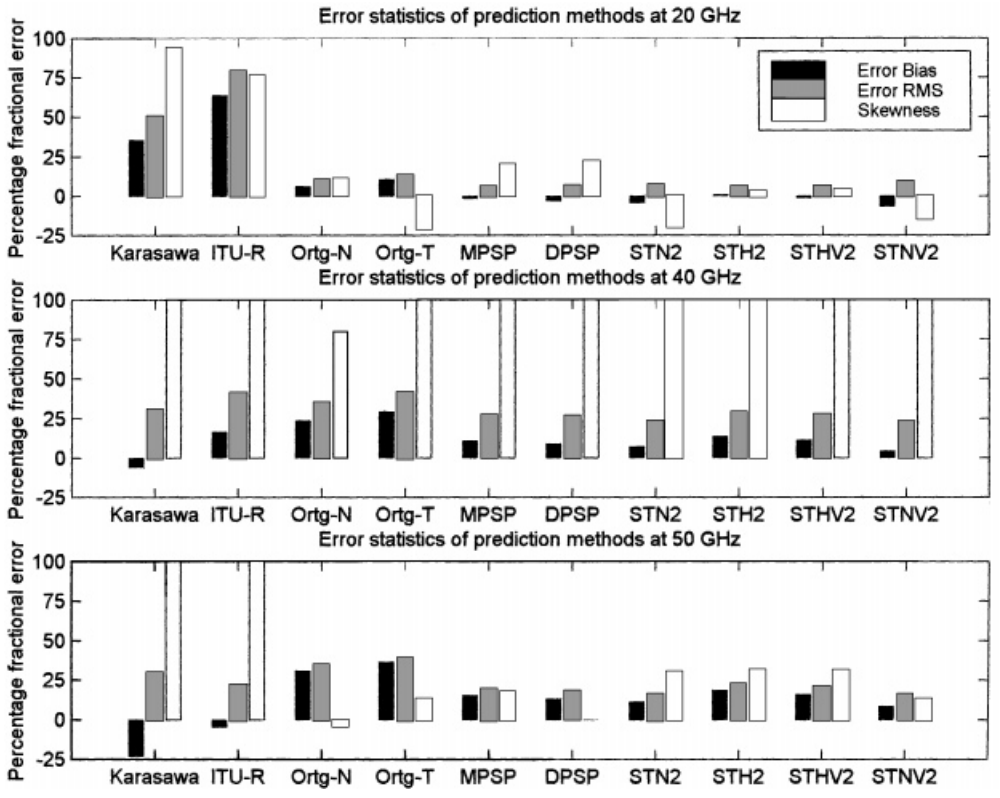

Figure 9. Bar diagram showing bias, rms value, and skewness of the percentage fractional error at 20 GHz (top panel), 40 GHz (middle panel), and 50 GHz (bottom panel) against the label of each considered prediction method. Skewness bars have been cut at 100 per cent (see Tables II–IV for values)

predictors can be developed using only easily achievable ground-based parameters as statistical inputs, as shown in this work and as in the case of the empirical methods. Of course, the results can be generalized to other geographical regions (where no RAOB stations are available) having similar climate conditions.

The main drawbacks of the model-based approach are represented, on the one hand, by the accuracy of the propagation model itself to represent the true scintillation phenomenon, and, on the other hand, by the temporal sampling of RAOBs which is generally limited to six hours. As said, the use of numerical weather forecast analyses at high temporal and spatial resolution, as meteorological vertical-profiles training data sets, could remove the latter limitation.

Scintillation predictions derived from six new statistical methods, based electromagnetic models applied to radiosounding observations and on multivariate regression analysis, have been compared with Italsat measurements at Spino d'Adda (Milan, Italy) acquired during 1995. Estimates derived from the empirical prediction methods of Karasawa, ITU-R and Ortgies have been also considered. After having statistically compared them with Italsat measurements in

terms of percentage error distributions, we can conclude that for this case study the model-based predictions can give fairly accurate estimates of scintillation variance and are at least comparable with the performances of the empirical methods. The interesting perspective to include into prediction methods a wider set of input parameters, like the vertically integrated water vapour content estimated from ground-based microwave radiometric measurements, has been also successfully tested in this work.

Future works should be aimed to enlarge the available Italsat data set for a more complete statistical assessment of the model-based methods, also including periods different from the chosen windows around midday and midnight. Moreover, the uncertainty in the knowledge of the frequency scaling exponent and its impact on the prediction method accuracy should be thoroughly investigated considering also various Italsat receiving sites.

Acknowledgements

This work has been partially supported by the Italian Ministry of University and Scientific and Technological Research (MURST) and the Italian Space Agency (ASI). We are grateful to Prof. A. Paraboni and Prof. G. d'Auria for their helpful suggestions during this work. Finally, we thank two anonymous reviewers for their careful reading of the paper and for their useful comments.

References

1. M. Filip and E. Vilar, 'Optimum utilization of the channel capacity of a satellite link in the presence of amplitude scintillations and rain attenuation', *IEEE Trans. Commun.*, **28**, 1958–1965 (1990).
2. P. A. Watson and Y. F. Hu, 'Prediction of attenuation on satellite-earth links for systems operating with low fade margins', *IEE Proc. Microwave Antennas Propagation*, **141**, 467–472 (1994).
3. E. T. Salonen, J. K. Tervonen and W. J. Vogel, 'Scintillation effects on total fade distributions for earth-satellite links', *IEEE Trans. Antennas Propagation*, **44**, 1–5 (1996).
4. E. Matricciani, M. Mauri and C. Riva, 'Relationship between scintillation and rain attenuation at 19·77 GHz', *Radio Sci.*, **31**, 273–279 (1996).
5. O. P. Banjo and E. Vilar, 'Measurements and modelling of amplitude scintillations on low-elevation Earth-space paths and impact on communication systems', *IEEE Trans. Commun.*, **34**, 774–780 (1986).
6. P. Basili, P. Ciotti, G. d'Auria, P. Ferrazzoli and D. Solimini, 'Case study of intense scintillation events on the OTS path', *IEEE Trans. Antennas Propagation*, **38**, 107–113 (1990).
7. D. L. Bryant, 'Low elevation angle 11 GHz beacon measurements at Goonhilly earth station', *BT Technol. J.*, **10**, 68–75 (1992).
8. G. De Angelis, A. Paraboni, C. Riva, F. Zaccarini, G. Dellagiacoma, L. Ordano, R. Polonio, M. Mauri and A. Pawlina, 'Attenuation and scintillation statistics with Olympus and Italsat satellites in Italy', *Alta Frequenza*, **6**, 66–69 (1994).
9. G. d'Auria, F.S. Marzano and U. Merlo, 'Model for estimating the refractive-index structure constant in clear-air intermittent turbulence', *Appl. Opt.*, **32**, 2674–2680 (1993).
10. F. S. Marzano and G. d'Auria, 'Estimation of intermittent scintillation on microwave links from meteorological data', *Alta Frequenza*, **6**, 94–97 (1994).
11. G. Peeters, F. S. Marzano, G. d'Auria, C. Riva and D. Vanhoenacker-Janvier, 'Evaluation of statistical models for clear-air scintillation using Olympus satellite measurements', *Int. J. Sat. Commun.*, **15**, 73–88 (1997).
12. F. S. Marzano and G. d'Auria, 'Model-based prediction of amplitude scintillation variance due to clear-air tropospheric turbulence along earth-satellite microwave links', *IEEE Trans. Antennas Propagation*, **46**, 1506–1518 (1998).
13. ITU-R, Report 718-3, 'Effects of tropospheric refraction on radio-wave propagation', *Reports of the CCIR on Propagation in non-ionized media*, Annex to Vol. V, Geneva (CH), 1990, pp. 172–176.
14. Y. Karasawa, M. Yamada and J. E. Allnutt, 'A new prediction method for tropospheric scintillation on earth-space paths', *IEEE Trans. Antennas Propagation*, **36**, 1608–1614 (1988).
15. G. Ortgies, 'Frequency dependence of slant-path amplitude scintillations', *Proc. 20th Meeting of Italsat propagation experiment* (*OPEX*), Darmstadt (Germany), 1993, pp. 156–164.
16. G. Ortgies, 'Prediction of slant-path amplitude scintillation from meteorological parameters', *Proc. Int. Symp. on Radio Propagation*, Beijing (China), 1993, pp. 218–221.

17. V. I. Tatarskii, *The effects of the turbulent atmosphere on wave propagation*, Israel Program for Scientific Translations, Jerusalem, 1971.
18. U. Merlo, E. Fionda and J. Wang, 'Ground level refractivity and scintillation in space-earth links', *Appl. Opt.*, **27**, 2247–2252 (1987).
19. F. S. Marzano, C. Riva, A. Banich, F. Clivio, G. d'Auria and A. Paraboni, 'Model-based prediction of amplitude scintillation variance in the 10–50 GHz band: comparison with Italsat satellite measurements', *Proc. First Int. Workshop on Radiowave Propagation Modelling for SatCom Services at Ku-band and above*, Noordwijk (The Netherlands), 28–29 October 1998.

Authors' biographies:

Frank Silvio Marzano was born in Jersey City, NJ, on May 3, 1963. He received the Laurea Degree (*cum laude*) in Electronics Engineering (1988) and the PhD degree (1993) in Applied Electromagnetics from the University 'La Sapienza' of Rome, Rome, Italy. In 1992 he has been visiting scientist at Florida State University, Tallahassee, FL and in 1993 he collaborated with the Institute of Atmospheric Physics, CNR, Rome, Italy. From 1994 till 1996, he has been with the Italian Space Agency and with the Department of Electronics Engineering of the University 'La Sapienza' of Rome, Rome, Italy, as a Post-doctoral researcher. After being a lecturer in 1997 at the University of Perugia, Perugia, Italy, he joined the Department of Electrical Engineering at the University of L'Aquila, L'Aquila, Italy where he is presently Assistant Professor. His researches mainly concern passive and active remote sensing of the atmosphere from airborne and spaceborne platforms, with a special focus on precipitation and inversion method development, radiative transfer modelling of scattering media and analysis of tropospheric scintillation along satellite microwave links. Since 1990 he has been involved in several international projects on remote sensing and telecommunications. Dr Marzano received the Young Scientist Award of XXIV General Assembly of the International Union of Radio Science (URSI) in 1993.

Carlo Riva was born in Monza, Italy in 1965. He received the Laurea Degree (*cum laude*) in Electronics Engineering from the Politecnico di Milano in 1990. From 1991 to 1994 he attended the Doctorate course in Electronics and Communication Engineering at the Politecnico di Milano in the propagation field with a special focus on scintillations. For three months in 1992 he was at European Space Research and Technology Centre, Noordwijk, The Netherlands, working on scintillation. In 1993 he was with the Universitè Catholique de Louvain, Louvain-la-Neuve, Belgium, for two months doing research on the separation of turbulence and rain effects on satellite communication links. He is currently with the Department of Electronics and Information, Politecnico di Milano, Milan, Italy as an Assistant Professor with a research task in millimetre-wave propagation.

Alessio Banich received the Laurea Degree in Communication Engineering in 1998 from the Politecnico di Milano, Milan, Italy with a thesis on the statistical prediction of scintillation along earth–satellite microwave links. Since April 1998 he has been collaborating with the Department of Electronics and Information of Politecnico di Milano, Milan, Italy on microwave scintillation topics.

Fabio Clivio obtained the Laurea Degree in Communication Engineering in 1998 from the Politecnico di Milano, Milan, Italy with a thesis on the statistical prediction of scintillation along earth–satellite microwave links. Since April 1998 he has been collaborating with the Department of Electronics and Information of Politecnico di Milano, Milan, Italy on topics related to scintillation analysis.

